Eur. Phys. J. D **32**, 139–146 (2005)
DOI: 10.1140/epjd/e2004-00179-x

THE EUROPEAN PHYSICAL JOURNAL D

A planar Penning trap

S. Stahl[1], F. Galve[1,2], J. Alonso[1,2], S. Djekic[1], W. Quint[2], T. Valenzuela[1], J. Verdú[1], M. Vogel[1,a], and G. Werth[1]

[1] Institut für Physik, Johannes-Gutenberg-Universität, 55099 Mainz, Germany
[2] GSI, 64291 Darmstadt, Germany

Received 4 May 2004 / Received in final form 9 August 2004
Published online 7 December 2004 –

Abstract. We present a new concept for a Penning trap, which is planar and allows for the implementation of novel confinement techniques. The trap provides confinement perpendicular to its plane by an electric potential minimum while a superimposed magnetic field provides radial confinement. Both the axial position and the depth of the potential minimum can be controlled by the applied voltages. The device is scalable in the sense that an arbitrary number of planar traps can be embedded in one plane thus representing a multitrap array which can be used for particle interaction studies. Switches between different traps in the planar array allow for controlled interactions between the single stored particles.

PACS. 85.35.Gv Single electron devices – 07.20.Mc Cryogenics and low temperature equipment – 07.50.-eElectronic instruments and components – 07.90.+c Other topics in instruments

1 Introduction

Penning traps confine charged particles by a combination of static electric and magnetic fields [1–3]. The electric field provides a potential minimum in one direction, commonly called the z-direction. The defocusing force of this field in the plane perpendicular to the z-axis is compensated by a magnetic field directed along the z-axis. When operated under ultra-high vacuum conditions virtually unlimited times for confinement of charged particles such as electrons and protons and their antiparticles as well as singly or multiply charged ions have been achieved. Penning traps have been successfully used in the determination of fundamental constants [4,5], high precision mass spectrometry [6–9], or Zeeman spectroscopy [10–12].

In a similar way their counterpart, the Paul trap, which uses only time varying electric fields to produce a time averaged potential minimum, has been applied to precision spectroscopy such as hyperfine measurements [13], lifetime determination of long lived metastable ionic energy levels [14–17], and the development of frequency standards [18]. More recently Paul traps have proven to be potentially useful tools in the development of quantum computation [19,20]. In this context planar Paul traps have been developed which offer interesting possibilities in the study of multipartite systems and entanglement [21].

In this article, we discuss the properties and possible applications of a planar Penning trap. We will first describe the general idea of this device in comparison to conventional Penning traps. A particular feature of planar Penning traps is the possibility of miniaturisation and the formation of 2D trap arrays, which may be useful when coupling of several single particles is the issue. Trap arrays and the coupling mechanism will be discussed in more detail in the third section of the paper.

2 Planar trap

A conventional 3D Penning trap consists of two electrically connected endcap electrodes at a distance $2z_0$ and one ring electrode of radius r_0. When the surfaces of the electrodes follow hyperboloids of revolution, the potential in the space between the electrodes depends on the square of the coordinates and therefore has a quadrupolar shape. It has the expression:

$$\Phi(x,y,z) = \frac{U}{2d_0^2}\left(x^2+y^2-2z^2\right) \qquad (1)$$

where U is the potential difference between ring and endcap electrodes and d_0 a characteristic trap dimension. The equation of motion of a charged particle in this potential can be solved analytically and is well-known to yield three eigenfrequencies, namely the cyclotron, axial and magnetron frequencies. When the electrode shape deviates from the hyperbolic form, the dependence of the potential on the coordinates will be different. As long as rotational symmetry with respect to the z-axis is preserved, the potential can easily be expanded in spherical harmonics and the leading term remains the quadrupole part.

Converting the three-dimensional electrode array into a two-dimensional one is achieved by removing the upper

[a] e-mail: manuel.vogel@uni-mainz.de

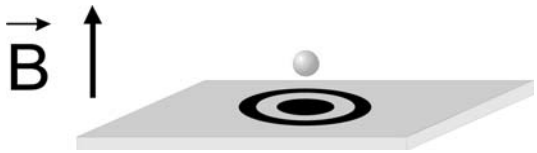

Fig. 1. Planar trap scheme. The electrodes (black) are embedded in a plane made of an isolator.

endcap and embedding the ring and lower endcap in a plane. The result is displayed in Figure 1. This is the simplest 2D configuration possible. Further ring electrodes may be added if necessary to enhance the properties of the trap. This case will be discussed in Section 2.1.

Mechanically the electrodes of a planar trap can be implemented by use of well-established thin film or thick film technology on a ceramic substrate, e.g. using gold as electrode material. Thick film technology has been in use since decades, giving spatial resolution in the order of 20 μm, whereas thin film technology achieves even sub-μm resolution. To avoid charge accumulation on the substrate and the corresponding disturbing influences on the trapping behavior, an additional surface layer of low conductivity can be used. Thin layers of e.g. graphite or gold in the high MΩ-region avoid a charging-up, yet isolate the electrodes sufficiently to avoid shortcuts. The electrodes are connected to the respective voltage supplies by contacts through the substrate.

In contrast to conventional Penning traps the planar trap represents an open geometry. This allows to access the trapped particles with any kind of radiation or beam and avoids to a large extent the occurrence of "cavity effects" which may affect the damping of the oscillation modes [22]. This is of particular importance for the cyclotron mode in the case of stored electrons. Moreover, the position of the trapped particles as well as the depth of the potential can be varied to a certain extent by appropriate choice of the applied voltages, as will be discussed below.

2.1 Shape of the trapping potential

The electrostatic potential for a fixed set of parameters exhibits a minimum at a well-defined distance above the trap's plane. This minimum serves for axial confinement of a charged particle, while radial confinement is assured by the magnetic field along the z-direction, as in conventional Penning traps.

The electrostatic potential can be generally expressed by the linear combination

$$\int_0^\infty dk\, \left(A(k)\, e^{-kz} + B(k)\, e^{kz}\right) \left(J_0(k\rho) + C(k) N_0(k\rho)\right)$$

with J_ν and N_ν being the standard Bessel functions of first and second kind, respectively [23]. In our case $\nu = 0$ because of cylindrical symmetry. Thus, a particle trapped in the region $z > 0$ feels a potential of the form

$$\phi(z,\rho) = \int_0^\infty dk\, A(k)\, e^{-kz} J_0(k\rho), \tag{2}$$

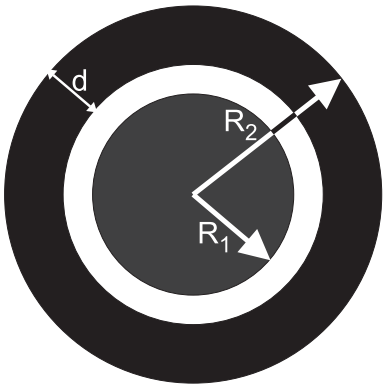

Fig. 2. Geometry parameters of the planar trap.

where the terms with $B(k)$, $C(k)$ have been dropped because they diverge for $z \to \infty$ and $\rho \to \infty$, respectively. In order to obtain the coefficients $A(k)$ we impose the values of the potential in the plane $z = 0$

$$V(\rho) \equiv \phi(0,\rho) = \int_0^\infty dk\, A(k)\, J_0(k\rho) \tag{3}$$

which, by use of the Hankel transform [23], allows for writing

$$A(k) = k \int_0^\infty d\rho\, \rho\, V(\rho)\, J_0(k\rho). \tag{4}$$

As $V(\rho)$ is piecewise constant, the coefficients $A(k)$ are a sum of the contributions from each electrode:

$$A(k) = \sum_i A_i(k) \tag{5}$$

with

$$A_i(k) = V_i \left[R_i J_1(kR_i) - (R_i - d_i) J_1\left(k(R_i - d_i)\right)\right] \tag{6}$$

where R_i denotes the distance at which electrode i ends and d_i its thickness. Thus, the central electrode ends at R_1, the inner ring electrode at R_2 and so forth (see Fig. 2).

Note, that for the step from equations (3) to (4) it is a necessary condition to have a well-defined voltage at every position on the surface $z = 0$, i.e. a real trap will deviate from this description due to gaps between electrodes and due to the finite size. Hence, a numerical comparison between the idealized potential given by the coefficients in equation (6) and a realistic one was performed. In the region of the potential minimum, i.e. in the region that determines the trapping behavior, the deviations were found to be negligible on the scale of precision as needed in the present investigations.

Based on the coefficients $A(k)$ one can integrate the potential in the whole space by using expression (2). As we are interested in confinement along the z-axis the desired solution is obtained by

$$\phi(z,0) \equiv \phi(z) = \int_0^\infty dk\, A(k)\, e^{-kz}, \tag{7}$$

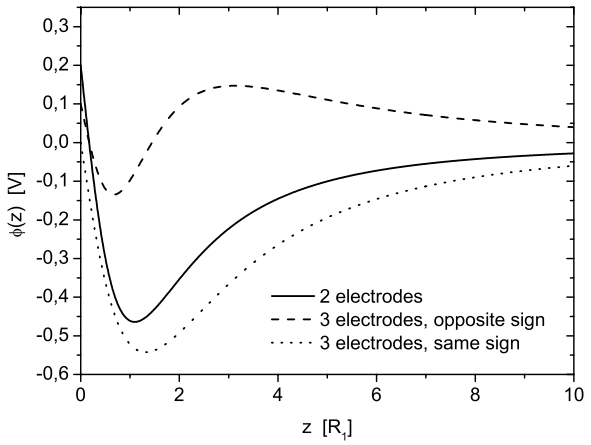

Fig. 3. Axial potential as a function of the axial position measured in units of the inner electrode radius for three distinct cases of applied voltages. For details, see text.

which is an analytic expression and represents a sum of contributions from each electrode of the type

$$\phi_i(z) = V_i \left(\frac{1}{\sqrt{1 + \frac{(R_i - d_i)^2}{z^2}}} - \frac{1}{\sqrt{1 + \frac{R_i^2}{z^2}}} \right). \qquad (8)$$

The potential in equation (8) describes a trap with as many adjacent electrodes as desired (one disk and many rings), but in this paper we will consider only the possibility of having either 2 or 3 electrodes plus an external ring electrode which is grounded and ensures that our approximation is sufficiently correct. The condition that the electrodes are adjacent can be written as

$$R_{i+1} = R_i + d_{i+1}.$$

In Figure 3, the resulting axial potentials for three simple choices of the electrode voltages are shown. The solid line represents the shape of the axial potential for the most simple case of two electrodes (central electrode and one ring electrode as shown in Fig. 2, $V_1 = 0.2$ V, $V_2 = -2$ V). The dotted line shows a case with an additional ring electrode outside the above configuration when the two ring electrodes have voltages of the same sign ($V_1 = 0$ V, $V_2 = -1$ V, $V_3 = -2$ V). Qualitatively, this configuration leads to the same potential shape as in the case with two electrodes, as one might expect. The dashed line gives the axial potential for the the same geometry, but with the two ring electrode voltages having opposite signs ($V_1 = 0.1$ V, $V_2 = -2$ V, $V_3 = 3$ V). In this case, both a maximum and a minimum occur. The shape of the minimum is changed as compared to the other configurations, affecting also the harmonicity, as will be discussed in the following section.

2.2 Harmonicity of the trapping potential

The established methods of detection and manipulation of trapped particles as relevant in the present case rely on well-defined motional frequencies. Presently, the axial frequency is of special interest. It is thus important to produce an axial trapping potential as harmonic as possible.

Let the anharmonicity be defined by the relative axial frequency difference between the particle at a finite motional energy and the ground energy $E_0 = \frac{1}{2}\hbar\omega_z$,

$$\kappa(E) := \frac{\omega_z(E) - \omega_z(E_0)}{\omega_z(E_0)}. \qquad (9)$$

Then the anharmonicity is given by

$$\kappa(E) = \sum_{i=1}^{\infty} [A(E)]^i \left| \frac{C_{i+2}}{2C_2} \right| \qquad (10)$$

with

$$A(E) = \sqrt{\frac{E}{m\omega_z^2}} \qquad (11)$$

being the motional amplitude of the particle along the z-direction and C_i being the coefficients of the electrostatic potential as expanded by

$$\phi(z) = \sum_{i=0}^{\infty} C_i (z - z_0)^i. \qquad (12)$$

A shift in axial frequency due to the anharmonicity of the trapping potential may obstruct a measurement of the corresponding signal. Detection of the particles' axial motion can be performed by pickup of the induced image current in the central trap electrode via a tuned resonance circuit of quality factor Q [29]. The width $\Delta\omega_z$ of the signal after transformation to the frequency domain is given by the inverse time cooling constant due to the resistivity R of the detection electronics. The cooling time constant is given by

$$\tau = \frac{mD^2}{q^2 R} \qquad (13)$$

where m is the particle mass, D is the effective distance of the particle to the electrode surface, q is the particle's charge. The resistance R is given by

$$R = \frac{Q}{\omega_z C}, \qquad (14)$$

where C is the parasitic capacitance of the detection electronics. For an electron trapped in a mm-scale planar trap at an axial frequency of 100 MHz with detection electronics of $Q = 300$ and $C = 7.5$ pF the width $\Delta\omega_z$ of the axial signal is around 1 kHz. The anharmonicity $\kappa(E)$ of the trapping potential needs to fulfill the relation

$$\kappa(E)\omega_z(E) \lesssim \Delta\omega_z. \qquad (15)$$

Thus, at an axial frequency of 100 MHz, anharmonicities κ in the 10^{-5} region are necessary to allow for a reliable measurement of the axial signal.

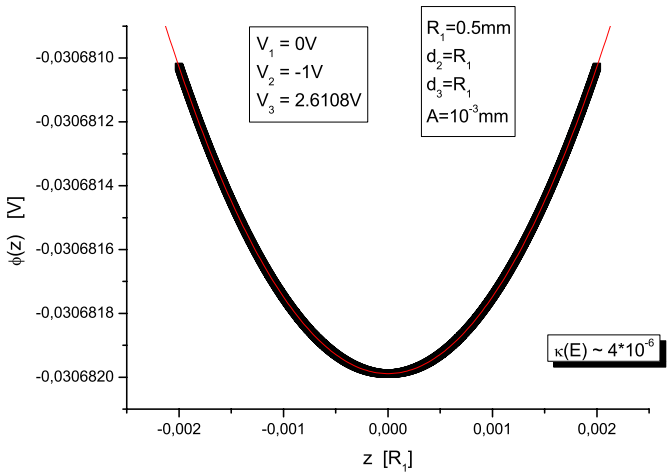

Fig. 4. Potential minimum in the range of an electron oscillating at $T = 100$ mK with $\omega_z \approx 100$ MHz. The electrode voltages have been chosen to $V_1 = 0$ V, $V_2 = -1$ V and $V_3 = 2.6108$ V.

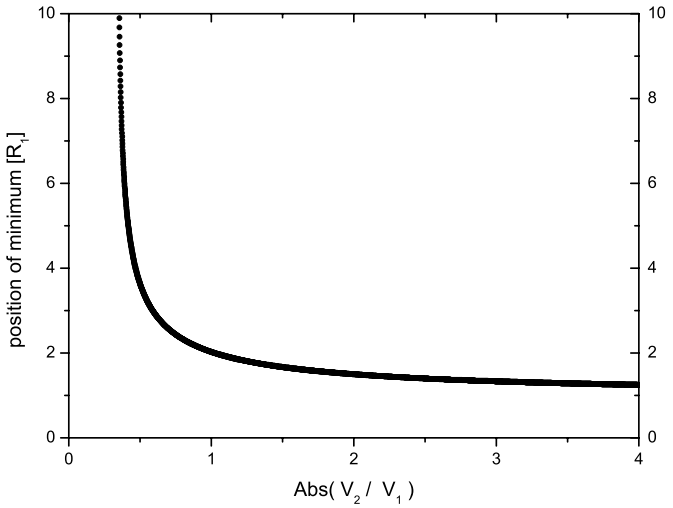

Fig. 5. Position of the potential minimum in units of the inner electrode radius as a function of the applied voltage ratio in the case with 2 electrodes.

An example of the shape of the trapping potential for a given choice of electrode voltages and geometries is given in Figure 4. It represents the potential minimum in the range of an electron oscillating at $T = 100$ mK with $\omega_z \approx 100$ MHz. The electrode voltages have been chosen to $V_1 = 0$ V, $V_2 = -1$ V and $V_3 = 2.6108$ V. A comparison of the calculated potential shape with a harmonic potential yields an anharmonicity κ of roughly 4×10^{-6}, which is sufficient for a reliable measurement of the axial signal.

2.3 Position of the minimum

For a given geometry the position of the potential minimum (z_0) can be chosen by the applied voltages. Even though an analytic solution for the potential function is known, the determination of its minimum implies solving a transcendental equation. It is thus necessary to extract this information numerically.

Figure 5 shows the case with two electrodes, in which the minimum distance z_0 is roughly given by the radius of the central electrode R_1. With three electrodes it is possible to shift the position of the minimum in a wider range. When the two ring voltages are of opposite sign, it is possible to change both the position of the minimum (by changing V_3 as compared to V_2) and also its depth (by changing the absolute values of both V_2 and V_3). This situation is displayed in Figure 6 for three choices of voltages leading to three different positions of the minimum z_1, z_2 and z_3. However, when the minimum is shifted towards $z = 0$, it narrows, causing the frequency of the axial motion to increase. One is therefore restricted to a range of distances which still allows for the particle to be detected by the corresponding tuned resonance circuit. This range is given by the width of the resonance circuit and the signal-to-noise ratio tolerable in the detection electronics. Nevertheless, since voltages can be controlled and stabilised on the millivolt level or below, the axial position of the stored particles can within the given range be

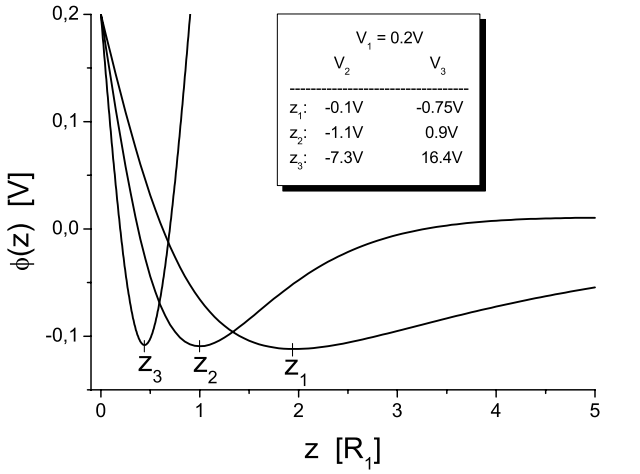

Fig. 6. Electrostatic potential as a function of z for three different choices of the applied voltages.

controlled with a high sensitivity. This will prove to be a great advantage when control over trap-trap interaction is desired, since the strength of the coupling depends on the position of the potential minimum. This will be discussed in further detail in Section 3.

2.4 Depth of the minimum

The depth of the potential minimum determines the maximum energy of the particles that allows for trapping. In the case with two electrodes it shows a linear dependence on the ring voltage and is of similar size. When three electrodes are being used, the overall linearity generally disappears and is replaced by regions of linearity interconnected by regions with different shape, depending on the exact positions and magnitudes of the superimposed potential contributions from different electrodes. Thus, the precise potential depth has to be evaluated in detail for

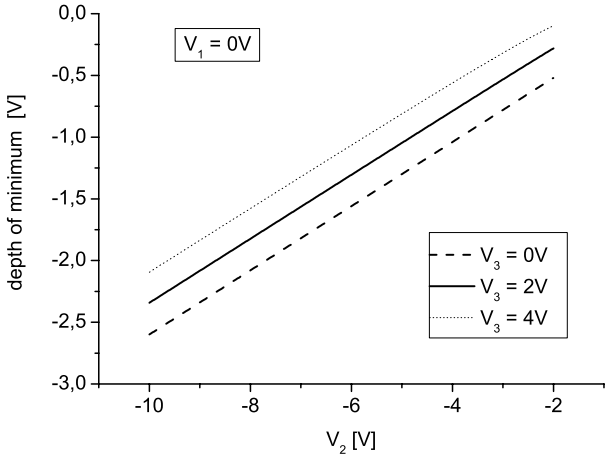

Fig. 7. Depth of the potential minimum as a function of the inner ring voltage V_2 for three cases of the outer ring voltage V_3 when the central electrode voltage is $V_1 = 0$ V.

the given set of parameters. Figure 7 shows the depth of the potential minimum as a function of the inner ring voltage V_2 for three cases of the outer ring voltage V_3 when the central electrode voltage is $V_1 = 0$ V. The behavior is nearly linear in each case, however the magnitude of the depth depends on the choice of V_3.

3 Trap-trap interaction

By connecting a pair of planar traps as sketched in Figure 8 one obtains a system of individually trapped, interacting particles. Each oscillating particle induces a charge in the central electrode of its trap which interacts via a connecting line with the other particle. This type of interaction has been studied before in [24,25], however, for the present purpose, a different approach is discussed. We assume that the induced charges are located on both surfaces of each central electrode and that the electrode thickness is negligible. Let the upper surfaces of the central electrodes have a common radius R and carry charges Q_1 and Q_2, respectively, while the remaining system, i.e. the two lower surfaces and the connecting wire, carries a common charge $Q_3 = -(Q_1 + Q_2)$. The classical Hamiltonian of this system is

$$H = H_1 + H_2 + q\frac{Q_1}{2\pi\epsilon_0 R^2}\left(\sqrt{R^2 + z_1^2} - z_1\right) + q\frac{Q_2}{2\pi\epsilon_0 R^2}\left(\sqrt{R^2 + z_2^2} - z_2\right) + \frac{Q_1^2}{2C_1} + \frac{Q_2^2}{2C_2} + \frac{Q_3^2}{2C_3}, \quad (16)$$

where q is the charge of a trapped particle, H_i are the particle Hamiltonians (which are effectively harmonic oscillators), C_i are the capacitances of the surfaces, and z_i is the axial positions of the particles.

If the induced charges are driven adiabatically by the oscillating particles (i.e. they are in every moment in equilibrium with the oscillating particle) we can write:

$$\frac{d(H - H_1 - H_2)}{dQ_i} = 0 \quad \forall i. \quad (17)$$

By applying this relation we obtain Q_1 and Q_2 as functions of the z_i, which inserted in the Hamiltonian (16) yields:

$$H = H_1 + H_2 + H_{int} \quad (18)$$

with H_{int} being a function of both z_i. The system can be quantised via the spatial variables of the axial oscillators, that is $z_i = z_0 + \tilde{z}_i$ where z_0 is the minimum of the axial electrostatic potential. The $\tilde{z}_i$ can be expressed with ladder operators describing the levels of the axial harmonic oscillator:

$$\tilde{z} \equiv \hat{z} = \sqrt{\frac{\hbar}{2m\omega}}\left(\hat{a} + \hat{a}^\dagger\right). \quad (19)$$

The Hamiltonian for the system in the interaction picture to first order in $\hat{z}_i$ and in terms of the ladder operators $\hat{a}_i^{(\dagger)}$ for each particle is:

$$\hat{H} = \hbar\omega_1\left(\hat{a}_1^\dagger\hat{a}_1 + \frac{1}{2}\right) + \hbar\omega_2\left(\hat{a}_2^\dagger\hat{a}_2 + \frac{1}{2}\right) + \hbar\omega_{int}\left(\hat{a}_1^\dagger\hat{a}_2 + \hat{a}_1\hat{a}_2^\dagger\right), \quad (20)$$

where the rotating wave approximation has been used and constant terms were removed. The quantised effective Hamiltonian describes the interchange of one photon at a rate ω_{int}. By use of the relations $C_1 = C_2 = \pi R\epsilon_0$ and $C_3 = 2C_1 + C_{wire} \sim 2C_1$, we obtain the expression for the interaction frequency:

$$\omega_{int} = \frac{q^2}{16\pi R^3\epsilon_0}\frac{1}{2m\omega_z}\left(1 - \frac{z_0}{\sqrt{R^2 + z_0^2}}\right)^2. \quad (21)$$

The interaction frequency is very sensitive to the length scales of the trap; to give an example, an electron confined in this configuration would have an interaction frequency

$$\omega_{int} \approx 10^2\frac{1}{\omega_z R^3}\left(1 - \frac{z_0}{\sqrt{R^2 + z_0^2}}\right)^2 \quad (22)$$

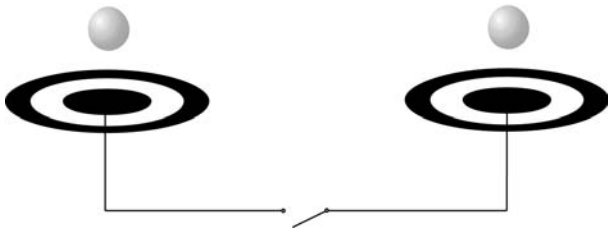

Fig. 8. Both traps are connected with a connection line, which enables the induced charges to exchange energy between different trapped particles. The interaction can be turned on and off by a switch.

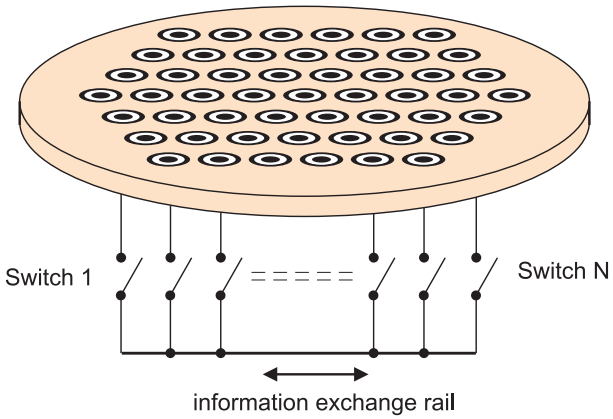

Fig. 9. Example of a 2D-array of planar traps connected by a switching matrix with an information exchange rail. A color version of the figure is available in electronic form at `http://www.eurphysj.org`.

with z_0, R given in meters and the frequencies given in Hz. If $z_0 \approx R$ and $R \approx 1$ mm then ω_{int} is of the order of $10^{10}/\omega_z$ s^{-2}, i.e. for an axial frequency of 1 MHz the effective interaction frequency is 10 kHz. If $R \approx 0.1$ mm then $\omega_{int} \approx 10^{13}/\omega_z$ s^{-2}, i.e. for an axial frequency of 1 MHz the interaction frequency is 10 MHz. The quantity in brackets in equation (22) gives the dependence on the distance z_0 and can vary the strength of the interaction by several orders of magnitude. For example, for $z_0/R = 1$ the quantity in brackets is about 0.1. Already for $z_0/R = 10$ the same quantity is 2×10^{-5}.

This means that even for a fixed trap geometry, it is still possible to control the speed of interaction within a certain range by moving the particles along the z-direction. This can be achieved via control of the position of the electric minimum, as described in Section 2.3. Note, that particle interaction does not rely on a connection line as it is assumed in the above discussion. Alternatively, one can also use the direct Coulomb interaction of the trapped particles and choose the interaction strength by geometric parameters and the detuning of the axial frequencies. Having both methods available can help studying which of them is more robust against decoherence.

4 Array of traps

One major advantage of the novel trap being planar is the possibility to arrange several traps in a plane. This would be the equivalent to the optical lattices used as multitraps in other experiments. The advantage compared to a possible linear array of Penning traps along the z-axis is due to the change from one spatial dimension (1D) to two (2D), since at a given length scale of order L, the number of traps in an array scales not with L, but with L^2. This opens up the possibility of implementing a large number of traps in parallel (Fig. 9).

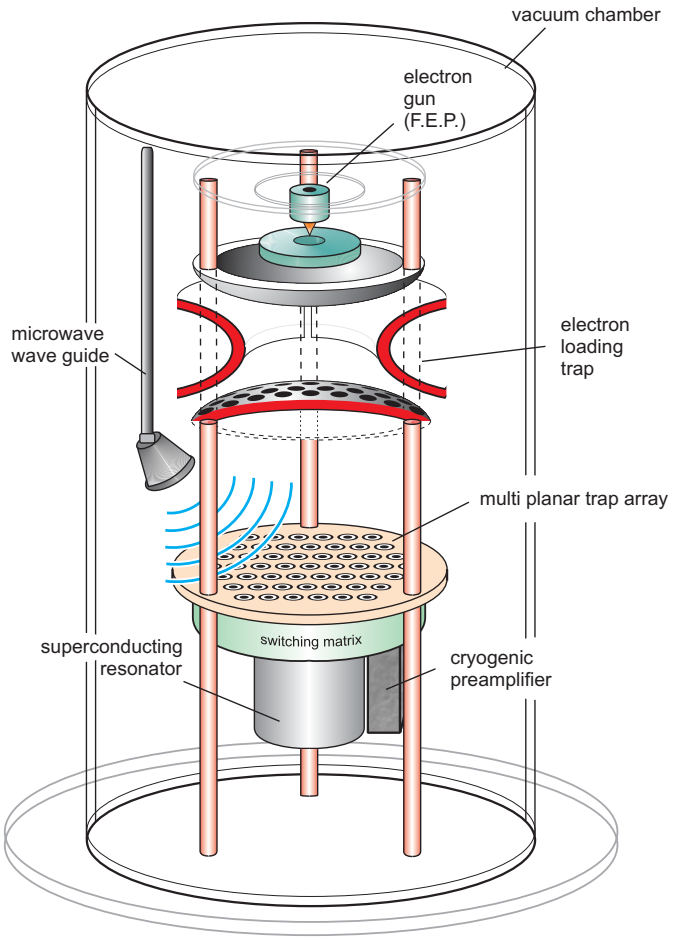

Fig. 10. Schematic representation of a possible setup with an array of planar traps used for trap-trap interaction studies on stored electrons. The interaction strength can be controlled by choice of the trap voltages and turned on and off by a switching matrix. A color version of the figure is available in electronic form at `http://www.eurphysj.org`.

5 Possible applications

Figure 10 shows a schematic representation of an experimental setup for an array of planar traps used for electron confinement. The set-up consists of a field emission point (FEP) as a source of electrons. A conventional hyperbolic Penning trap with a mesh as lower endcap is used for storage and preparation of the electrons to be trapped in the planar trap array. It is used to create a "shower" of a large number of electrons ($\approx 10^9$) onto the planar array by appropriate pulsing of the ring electrode voltage. Even with a capture efficiency of less than 10^{-4} it will thus be possible to trap some 10^3 electrons per trap. This number may then be lowered to one by use of well-established mechanisms (see e.g. [26]). Coupling of a number of single electrons may be performed by use of a switching matrix. A microwave source can be used in order to induce spin flips of the electron spin. When the device is used in a cryogenic surrounding, synchrotron radiation in the cyclotron motion of the electrons in the external magnetic field of several Tesla strength provides fast cooling of the

cyclotron motion [27]. By coupling of the cyclotron degree of freedom to the axial motion, also the axial degree of freedom can be cooled efficiently [28].

Detection of the electron's motion in a trap is achieved by detection of the image charge induced in the trap electrodes and the corresponding image current through the attached electronics [29]. A Fourier transform of the detected signal then yields the motional frequencies. The detection can be performed separately for the different motional degrees of freedom of the electron in analogy to similar measurements performed on single stored ions [26,28,30].

5.1 Single-particle measurements in parallel

It is commonly known that numerous experiments concerned with spectroscopy, atomic state lifetime measurements, mass- and g-factor precision measurements, frequency standards and many more gain substancially from employing trapping techniques. However, typically only one measurement is performed at a time since only one trap and/or one particle is employed. Planar traps may add some features to these kinds of investigations, since a 2D array of planar traps can be used for a simultaneous measurement of the same particle property in a large number of identical particles that are trapped and addressed individually. Measurement statistics is thus increased proportionally to the number of traps in use, limited virtually only by miniaturisation and electronics. Problems may arise from inhomogeneities of the magnetic field leading to slightly different values of the field strength in different traps. Field inhomogeneities of superconducting solenoids are typically as small as $\mu\mathrm{T/mm}^2$ or below, but might still influence high-precision measurements. However, a number of measurements is not sensitive to the absolute value of the field strength since only frequency ratios are measured, see e.g. the g-factor precision measurements as described in [26,28]. In these cases a shortening of the necessary measurement time by a factor $\sqrt{n}$ when n is the number of parallel measurements would be most welcome since it could help to reduce measurement time from months to weeks or to reduce the statistical uncertainty accordingly.

5.2 Single-trap quantum logic and controlled particle interaction

It has recently been achieved to implement quantum informational gates and algorithms with trapped ions [19,20,31–33]. The control over trapped particles and the natural long coherence time that a trap provides to quantum superpositions makes this tool desirable for developments in the field. It has recently also been proposed to use stored electrons for quantum information processing [34,35]. When a planar trap array is used for storage of single electrons at sufficiently low temperature, it appears possible to perform quantum logic with each single trapped electron as described in detail in [34,35], with two qubits per trap comprising two internal (spin) states and the external (quantized motion) states, preferably the ground state and the first excited state of the axial and cyclotron motion. Under the present conditions, at ambience temperatures below 100 mK as reached in ^{3}He–^{4}He dilution refrigerators, the electronic synchrotron radiation brings the electron into the ground state of the cyclotron motion [22]. The ground state of the axial motion may then be reached by coupling of the two motions. Control over the the spin state is assured by the possibility of inducing a spin flip by irradiation of appropriate microwaves. Detection of the spin state is performed by use of the "Continuous Stern-Gerlach effect" which measures the spin state by the corresponding axial frequency (for details on this technique see, e.g. [26,28]). Note, that the resonance circuit detecting the axial motion is switched off during logic operation so that the spin coherence is not affected; readout is applied only at the end.

The present Penning trap design yields furthermore the possibility to employ an array of single-electron traps with switchable interconnections between individual traps. The control over the interaction strength (or speed) of particles in different traps allows for studies of interaction effects and controlled coupling of different motional degrees of freedom of the particles. The interconnection of a number of one-electron two-qubit systems might make it possible to implement also quantum registers and error correction strategies as described in [34,35].

6 Conclusions

We have proposed a design for a planar Penning trap which can be scaled down to the sub-mm range. We have shown that the design allows for particle trapping and control over the position and the depth of the potential minimum by choice of the applied voltages. An arbitrary number of such traps may be arranged on a substrate chip and connected by cryogenic switches. The fact that an arbitrary number of traps can be arranged in 2D is an advance in the scalability of trapping devices. It has in addition the virtue of allowing for a number of parallel measurements of the same quantity in the study of single-particle properties, which increases the statistical significance of any observable. The possibility of a controlled interaction between different traps by use of a switching matrix provides a powerful tool for particle interaction studies.

We acknowledge stimulating discussions with P. Tombesi and coworkers. This work was funded by the BMBF and the EU in the framework of the QUELE project (grant no. FP6-003772).

References

1. F.M. Penning, Physica **3**, 873 (1936)
2. P.K. Ghosh, *Ion traps*, International series of monographs on physics 90 (Clarendon Press, Oxford 1995), ISBN: 0-19-853995-9

3. L.S. Brown, G. Gabrielse, Rev. Mod. Phys. **58**, 233 (1986)
4. R.S. Van Dyck, P.B. Schwinberg, H.G.Dehmelt, Phys. Rev. Lett. **59**, 26 (1987)
5. T. Beier et al., Phys. Rev. Lett. **88**, 011603 (2002)
6. F.L. Moore, D.L. Farnham, P.B. Schwinberg, R.S. Van Dyck, Nucl. Instr. Meth. B **43**, 425 (1989)
7. E.A. Cornell et al., Phys. Rev. Lett. **63**, 1674 (1989)
8. G. Bollen, R.B. Moore, G. Savard, H. Stolzenberg, J. Appl. Phys. **68**, 4355 (1990)
9. C. Gerz, D. Wilsdorf, G. Werth, Z. Phys. D **17**, 117 (1990)
10. G. Tomaseo et al., Eur. Phys. J. D **25**, 113 (2003)
11. D.J. Wineland et al., Phys. Rev. Lett. **50**, 628 (1983)
12. J. Verdú et al., Phys. Rev. Lett. **92**, 093002 (2004)
13. G. Savard, G. Werth, Ann. Rev. Nucl. Part. Sci. **50**, 119 (2000)
14. M. Knoop et al., Eur. Phys. J. D **30**, 163 (2004)
15. M. Block, O. Relm, P. Seibert, G. Werth, Europhys. Lett. **33**, 595 (1996)
16. P.A. Barton et al., Phys. Rev. A **62**, 032503 (2000)
17. P. Staanum et al., Phys. Rev. A **69**, 032503 (2004)
18. P. Gill et al., Meas. Sci. Technol. **14**, 1174 (2003)
19. D.J. Wineland et al., Phil. Trans. Roy. Soc. Lond. A **361**, 1349 (2003)
20. F. Schmidt-Kaler et al., Appl. Phys. B **77**, 789 (2003)
21. D. Kielpinski, C.R. Monroe, D.J. Wineland, Nature **417**, 709 (2002)
22. S. Peil, G. Gabrielse, Phys. Rev. Lett. **83**, 1287 (1999)
23. M. Abramowitz, A. Stegun, *Pocketbook of mathematical functions* (Frankfurt/Main, 1984)
24. D.J. Heinzen, D.J. Wineland, Phys. Rev. A **42**, 2977 (1990)
25. A.S. Sørensen et al., Phys. Rev. Lett. **92**, 063601 (2004)
26. G. Werth, H. Häffner, W. Quint, Adv. At. Mol. Opt. Phys. **48**, 191 (2002)
27. S. Djekic et al., Eur. Phys. J. D **31**, 451 (2004)
28. H. Häffner et al., Eur. Phys. J. D **22**, 163 (2003)
29. D.J. Wineland, H. Dehmelt, J. Appl. Phys. **46**, 919 (1975)
30. M. Diederich et al., Hyp. Int. **115**, 185 (1998)
31. J.I. Cirac, P. Zoller, Phys. Rev. Lett. **74**, 4091 (1995)
32. Q.A. Turchette et al., Phys. Rev. Lett. **81**, 3631 (1998)
33. D. Leibfried et al., Nature **422**, 412 (2003)
34. S. Mancini, A. Martins, P. Tombesi, Phys. Rev. A **61**, 012303 (2000)
35. G. Ciaramicoli, I. Marzoli, P. Tombesi, Phys. Rev. A **63**, 052307 (2001)